Separation and Purification Technology 73 (2010) 100–105

Contents lists available at ScienceDirect

Separation and Purification Technology

journal homepage: www.elsevier.com/locate/seppur

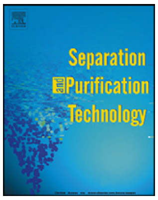

Simulation of a modified cyclone separator with a novel exhaust

Jihui Chen*, Xu Liu

Utilities Department, CISDI Engineering Co. Ltd., Chongqing 400013, PR China

ARTICLE INFO

Article history:
Received 23 December 2009
Received in revised form 10 March 2010
Accepted 11 March 2010

Keywords:
Cyclone separator
Separation efficiency
Pressure drop
Exhaust

ABSTRACT

Simulations on the separation efficiency and the pressure drop of a modified cyclone separator with a novel exhaust under different insert depths (250 mm, 350 mm, 450 mm, and 550 mm), sloping orientations (0°, 90°, 180°, and 270°), contracting angles (15°, 30°, and 45°) and sloping angles (5°, 10°, and 15°) were performed by computational fluid dynamics technique in this study. Results indicate that despite the pressure drop increases to some extent, the separation efficiency of such separators fundamentally exceeds that of the traditional linear-pipe-shaped ones due to the configuration of the novel exhaust can be made to harmonize with the flow field within the separator. Both the separation efficiency and the pressure drop change with the sloping orientation, and they have the same changing rule, the maximum at 90° and the minimum at 270°. The separation efficiency increases firstly and then decreases with increasing insert depth of the novel exhaust, and the maximum appears when the insert depth is 450 mm. The separation efficiency of the modified separator is about 4.6–7.9% higher than that of the traditional one under different sloping angles and contracting angles. Simulation results agree relatively well with the previous experimental results. Besides, based on an overall consideration of separation efficiency and pressure drop, we think that it is the most economic condition when the contracting angle is 30°. However, the contracting angle of 45° is still more suitable when the key problem is the separation efficiency despite its largest resistance loss.

1. Introduction

Circulating fluidized bed (CFB) combusting technology has developed fast during the last three decades and is widely used in the world due to its good characteristics such as satisfactory desulfurization efficiency, low NOx emission and suitability for different types of fuels [1]. As a key equipment for CFB boilers, gas–solid cyclone separator, which helps the circulation of the solids in the furnace, has strong effects on the combustion efficiency, the circulation rate, the desulfurization efficiency, and so on [2]. As we know, the size of cyclone separators increases rapidly with increasing the capacity of CFB boilers. However, large cyclone not only results in some manufacturing, installation and operation problems, but also has lower separation efficiency [3].

In recent years, experimental and theoretical investigations have been conducted in order to achieve the less size and higher separation efficiency of the gas–solid cyclone separators. The France's Stein Corporation developed a cyclone separator with an offset mounted exhaust [4]. Germany Siemens Corporation developed a cyclone separator with guide vanes at the top of the separator [5]. A novel double-inlet square cyclone separator with two furnaces developed by Clean Coal Combustion Laboratory of Chongqing University is very suitable to the scale-up of the CFB boilers [6]. A type of square cyclone separator with downward exhaust was developed and granted a Chinese patent [7]. Its separation efficiency was shown as good as that of the traditional cyclone of circular cross-section separator and its particle cut-diameter is about 15 μm. Moreover, researchers have carried out many investigations on the effect of cylinder height and diameter, the cone opening size, the exhaust diameter, length, insert depth, offset and turbulence intensity and boundary layer on the separator performance [8–17]. These results lay important foundations for optimizing and scale-up of cyclone separators.

As we know, however, the inside flow field of a single-inlet cyclone separator has not axial symmetry. The tangential velocity and the radial velocity at different angles in cyclone separator are also not uniform [18,19]. Thus, the shape of exhaust will have an influence on the flow and on the separation efficiency and pressure drop of cyclone separator.

In the previous work, experimental investigations have been carried out on the influence of the bottom-contracted and edge-sloped exhaust on the separation efficiency and the pressure drop of a cyclone separator under different insert depths and sloping orientations in a visual cold large-scale CFB setup [2].

---

* Corresponding author. Tel.: +86 23 63547546; fax: +86 23 63548888.
E-mail address: chenjihui_zl@yahoo.com (J. Chen).

1383-5866/$ – see front matter © 2010 Elsevier B.V. All rights reserved.
doi:10.1016/j.seppur.2010.03.007

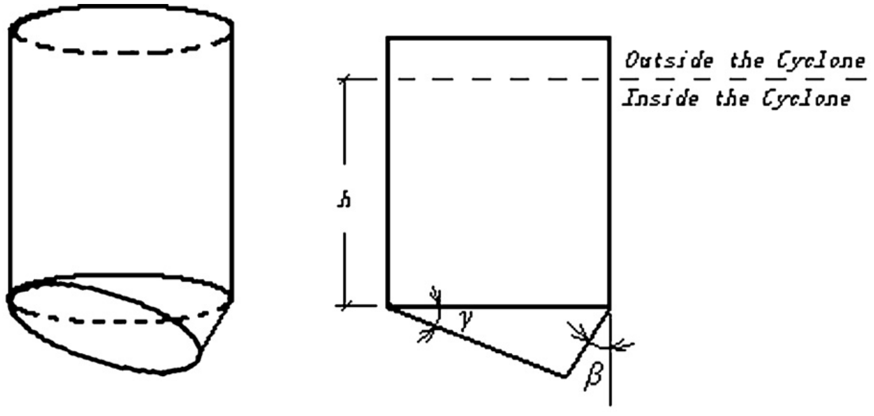

(a) the novel vent-pipe (b) the descriptions of sloping angle and contracting angle of the novel vent-pipe

Fig. 1. Schematics of the novel exhaust.

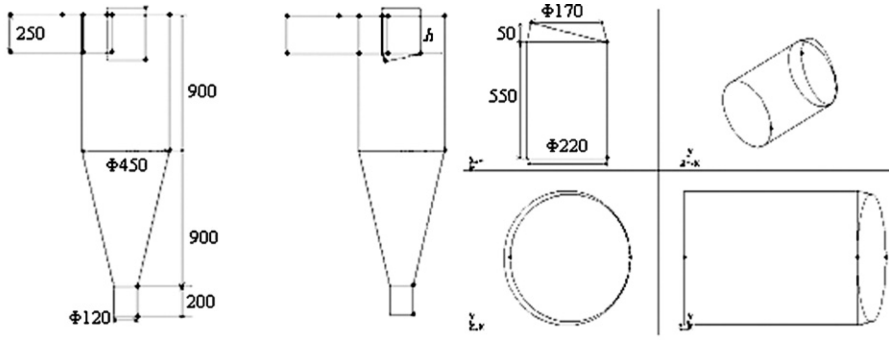

(a) the traditional cyclone (a) the modified cyclone

Fig. 2. The geometric models of two cyclones.

In order to validate the experimental results and comprehensively examine the performance of the modified cyclone separator with the novel exhaust, simulations were performed by computational fluid dynamics technique in this study.

2. Task formulation and numerical method

In the present work, the effect of a novel exhaust on the separation efficiency and pressure drop of a modified cyclone separator under different exhaust insert depths (250 mm, 350 mm, 450 mm, and 550 mm), sloping orientations (0°, 90°, 180°, and 270°), contracting angles (15°, 30°, and 45°) and sloping angles (5°, 10°, and 15°) will be studied in a CFB system. Besides, all the results will be compared with that of the traditional cyclone separator.

2.1. Geometric model

It should be pointed out that the sloping orientation represents the angle between the two directions of the sloped edge and the inlet stream. And the angle is described in clockwise when looking down the exhaust. The modified exhaust and the description of contracting angle and sloping angle of the exhaust can be seen in Fig. 1. In addition, the three-dimensional geometric models of two cyclones are shown in Fig. 2.

2.2. Mathematic model

(1) Governing equations for continuous phase

Continuity equation:

$$\frac{\partial \rho}{\partial t} + \frac{\partial}{\partial x_i}(\rho \nu_i) = 0 \tag{1}$$

Momentum equations:

$$\frac{\partial}{\partial t}(\rho \nu_i) + \frac{\partial}{\partial x_j}(\rho \nu_i \nu_j) = -\frac{\partial p}{\partial x_j} + \frac{\partial}{\partial x_j}\left[\mu\left(\frac{\partial \nu_i}{\partial x_i} + \frac{\partial \nu_j}{\partial x_j} - \frac{2}{3}\delta_{ij}\frac{\partial \nu_i}{\partial x_i}\right) - \frac{\partial(\rho \overline{\nu'_i \nu'_j})}{\partial x_{ji}}\right] \tag{2}$$

Reynolds stress model:

$$\frac{\partial(\rho \overline{\nu'_i \nu'_j})}{\partial t} + \frac{\partial(\rho \nu_k \overline{\nu'_i \nu'_j})}{\partial x_k} = D_{ij} + p_{ij} + \phi_{ij} - \varepsilon_{ij} \tag{3}$$

where $p_{ij} = -\rho\left(\overline{\nu'_i \nu'_k}\frac{\partial \nu_j}{\partial x_k} + \overline{\nu'_j \nu'_k}\frac{\partial \nu_i}{\partial x_k}\right)$, $D_{ij} = \frac{\partial}{\partial x_k}\left(\frac{\mu_t}{\sigma_k}\frac{\partial \overline{\nu'_i \nu'_j}}{\partial x_k}\right)$,

$p_{ij} = -\rho\left(\overline{\nu'_i \nu'_k}\frac{\partial \nu_j}{\partial x_k} + \overline{\nu'_j \nu'_k}\frac{\partial \nu_i}{\partial x_k}\right)$, $\phi_{ij} = \phi_{ij1} + \phi_{ij2}$, $\phi_{ij1} = -C_1 \rho \frac{\varepsilon}{k}\left(\overline{\nu'_i \nu'_j} - \frac{2}{3}\delta_{ij} k\right)$,

$\phi_{ij2} = -C_2\left(p_{ij} - \frac{2}{3}\delta_{ij} G_k\right)$, $G_k = -2\rho \overline{\nu'_i \nu'_k}\frac{\partial \nu_i}{\partial x_k}$, and $\varepsilon_{ij} = \frac{2}{3}\delta_{ij}\rho\varepsilon$

$$\frac{\partial}{\partial t}(\rho k) + \frac{\partial}{\partial x_j}(\rho \nu_i k) = -\frac{\partial}{\partial x_j}\left[\left(\mu + \frac{\mu_t}{\sigma_k}\right)\frac{\partial k}{\partial x_j}\right] + \frac{1}{2}(P_{ij} + G_{ij}) - \rho\varepsilon \tag{4}$$